THE ASTRONOMICAL JOURNAL VOLUME 110, NUMBER 1 JULY 1995

STUDY OF DEEP *IRAS* FIELDS AT 60 μm

D. T. GREGORICH
Infrared Processing and Analysis Center (IPAC), California Institute of Technology, Pasadena, California 91125, and Department of Physics, California State University, Los Angeles, California 90032
Electronic mail: dtg@ipac.caltech.edu

G. NEUGEBAUER
Palomar Observatory, California Institute of Technology, 320-47, Pasadena, California 91125
Electronic mail: gxn@caltech.edu

B. T. SOIFER
Palomar Observatory, California Institute of Technology, 320-47, Pasadena, California 91125
Electronic mail: bts@mop.caltech.edu

J. E. GUNN[1]
Princeton University Observatory, Princeton, New Jersey 08544
Electronic mail: jeg@astro.princeton.edu

T. L. HERTER
Cornell University, 212 Space Sciences Bldg., Ithaca, New York 14853
Electronic mail: herter@astrosun.tn.cornell.edu

Received 1995 January 25; revised 1995 March 14

ABSTRACT

A selected subset of *IRAS* pointed observations has been examined to study infrared galaxies at 60 μm in the 50 to 100 mJy range. The observations cover a total area of 20 sq° and contain a total of 746 sources with signal to instrumental noise ratios SNR >5. Detailed observations of one of these fields at visual, near-infrared, radio and x-ray wavelengths indicate that these sources, the faintest extracted from the *IRAS* data, are dusty galaxies much like the bulk of infrared galaxies observed by *IRAS*. The area covered triples, in 20 different fields, the area of the previously most sensitive *IRAS* survey of sources in this flux density range. The number of sources is about seven times that previously extracted, and the source density is about twice that found in the previous study at this flux level. The observed 60 μm source counts are consistent with an evolutionary model of the number of infrared luminous galaxies that fits the observed radio source counts; the counts are inconsistent with a nonevolutionary model. © *1995 American Astronomical Society.*

1. INTRODUCTION

The *IRAS* survey reached a range of sensitivity levels which depend on the area covered and the processing of the observations. The original all-sky survey has sensitivity limits for point sources of around 500 mJy at 12, 25, and 60 μm and 1.5 Jy at 100 μm (Beichman *et al.* 1985). The Faint Source Survey (FSS), which resulted from further processing of the observations, reached sensitivity limits of 200 mJy at 12, 25, and 60 μm and 1 Jy at 100 μm (Moshir *et al.* 1992). Hacking & Houck (1987, hereafter referred to as HH) describe a restricted survey of the 6.25 sq° area near the North ecliptic pole which included both survey scans and special calibration scans made at half the scan speed of the survey scans that achieved a flux density limit at 60 μm of $f_\nu(60\ \mu\text{m}) \sim 50$ mJy and included 98 sources.

At its faintest limits, the *IRAS* survey can be used to investigate if the properties of galaxies at cosmologically interesting distances have evolved over time. Hacking *et al.* (1987, hereafter referred to as HCH) concluded that the number counts of faint *IRAS* galaxies derived from HH were inconsistent with a nonevolving universe, although the number counts were lower by a factor close to 2 than expected from counts at radio wavelengths. This analysis was supplemented by Saunders (1990) and Lonsdale *et al.* (1990) who showed that the number counts derived from the FSS tied smoothly into those of HCH.

Faint sources can be studied through an analysis of the *IRAS* Pointed Observations. These observations were taken in multiples of 15 min duration and typically reached a limiting flux density five to ten times below that achieved in the survey proper (Young *et al.* 1985). Lonsdale & Hacking (1989) and Elias *et al.* (1993) have used pointed observations in conjunction with ground based optical spectroscopy to investigate galaxies with 60 μm flux densities in the 100 to 400 mJy range; both sets of authors again find that some galaxy evolution is necessary. In this paper, a selected subset of the *IRAS* pointed observations is examined to study infra-

[1]Visiting Associate, Palomar Observatory, California Institute of Technology.

 0004-6256/95/110(1)/259/9/$0.90

TABLE 1. *IRAS* FL mode observations with more than eight scans.

FL Field	Ra 1950 h m	Dec 1950 ° '	Galactic latitude °	Coverage scans	Area Covered sq °	60 μm Noise mJy	Number 60 μm sources[a]
15	0 13.6	-55 27.0	-60	20	0.82	12	20
11	3 23.0	-71 34.8	-40	145	1.51	3	33
2	3 39.0	-77 15.0	-36	61	1.49	5	36
42	4 11.0	-62 48.0	-41	33	0.70	6	25
63	4 26.0	-55 21.0	-42	64	1.15	6	27
50	5 6.0	-56 18.0	-36	53	1.06	7	25
117	6 0.0	-54 42.0	-28	68	1.34	5	33
122	6 2.0	-81 30.0	-28	60	1.16	5	39
125	6 46.0	+74 27.0	+26	63	1.06	5	33
16	9 33.0	-14 25.2	+26	10	0.61	11	18
60	15 7.0	+33 18.0	+59	12	0.69	11	13
55	16 11.0	+ 4 30.0	+36	17	0.81	9	17
73	16 41.0	+39 57.0	+41	8	0.49	13	12
66	16 52.0	+39 52.8	+38	12	0.71	10	20
29	17 7.0	+71 10.2	+33	53	1.25	6	32
113	17 27.0	+50 15.0	+33	14	0.71	12	9
123	18 1.0	+51 30.0	+28	23	0.94	9	19
71	18 7.0	+69 52.8	+29	69	1.31	5	58
115	18 46.0	+79 45.0	+27	38	1.10	7	28
4	21 47.0	-67 30.0	-41	53	1.10	7	29

Comments
a) SNR > 5
$f_\nu(60\ \mu m) > 50$ mJy

red galaxies in the 50 to 100 mJy range over a large solid angle and widely distributed pointings.

2. OBSERVATIONS—THE *IRAS* FILLER POINTED OBSERVATIONS

In general, the duration of each of the *IRAS* pointed observations was 15 min. Often, constraints in the survey strategy, which had first priority in the *IRAS* mission, resulted in timing gaps which did not correspond to integral number of 15 min intervals and thus observing time was potentially lost. In order to avoid this loss, a mode of pointed observation, the "filler" or FL mode, was created after the start of the *IRAS* mission. The targets of the observations in this mode were arbitrary and were relatively uniformly distributed over the sky in ecliptic coordinates and the spacecraft was pointed at the nearest FL target whenever it was otherwise not busy.

Each FL observation consisted of three or four scans either 50′ or 100′ long which were offset by 0.8′ from each other. The position angles of the scans were defined by the position of the *IRAS* satellite relative to the Earth and Sun. The coverage of a target field was therefore time dependent throughout the *IRAS* mission and sequential observations potentially mapped the target with different position angles in the sky; multiple observations generally filled in an area of about 1 sq° around the target. The command sequences which defined the FL observations are described in detail by Young *et al.* (1985).

From 1984 May through 1984 November there were 1729 separate FL observations of 66 fields. The depth of coverage at any one field ranged from 1 to 145 observations; 41 FL fields had eight or more observations of a given area. These fields are singled out because eight observations generally achieved a limiting flux density $f_\nu(60\ \mu m)$ due to instrumental noise of around 10 mJy (1σ).

The sample used in the present paper consists of a subset of the filler fields with an absolute Galactic latitude $|b| > 25°$. This constraint was chosen to reduce the contamination by Galactic "cirrus" (Low *et al.* 1984) and yet to retain a significant area coverage; it reduces the sample to 20 fields. All but one of the 20 selected fields were in areas designated with "moderate cirrus" or "low cirrus" flags in the FSS catalog. One was designated with a "high maximum FSS cirrus" flag, but was otherwise not exceptional. For reference, the field studied by HH was at $b = 30°$ and is designated of "moderate cirrus." The characteristics of the sample fields are given in Table 1. The area of each field was a function of the noise level attained, essentially a function of the coverage; see the discussion in HH and FSS. For example, the total area with a 5σ sensitivity of 100 mJy was 20 sq° for the 20 fields sampled; the area of individual fields varied from a low of 0.6 sq° to a high of 1.5 sq°. The quantity listed in Table 1 as "area" gives the limiting area for high flux densities (~350 mJy) in each field.

3. DATA PROCESSING

The data were reduced in a manner very similar to that described in detail in HH, and most of the issues considered by HH apply to the FL dataset. Specifically, each detector track was first filtered using a zero sum filter; an example of a filtered image is shown in the Appendix. The main difference between the analysis of HH and the present one is in the method of computing the noise so that accurate, automated extractions based on signal to noise ratios could be carried out. When the HH coaddition weights were applied to observations containing only pointed observations, the improvement in the signal to noise ratios predicted with additional images was not achieved. The data used by HH incorporated survey like scans which smoothed the sky coverage and masked this problem. A coverage-based noise algorithm was therefore developed and applied to the FL dataset.

In order to automate the process of source extraction, a source extraction and coaddition algorithm similar to that used for the FSS was designed and implemented. A separate coverage file was maintained for each pixel in the area scanned, and detector crossings were coadded with equal weights for each scan, rather than, e.g., weights dependent on some intrinsic detector noise. Pixels with less than eight coverages were not considered, and the "instrumental noise" was derived on the basis of comparisons between multiple crossings over one pixel.

Because the present data were analyzed using new software, the data of the North ecliptic pole field studied by HH were reanalyzed; the results of the present analysis were entirely consistent with the HH analysis. In addition, a visual inspection of each source extracted in the central portion of one field (FL29) indicated that the extraction technique was performing satisfactorily and that the noise behaved as anticipated.

4. RESULTS

The 20 FL fields characterized in Table 1 were each scanned at least eight times. They cover a total area of 20.0 sq° and contain a total of 746 sources with signal to instrumental noise ratios at 60 μm SNR >5. Of this total, 526 sources have $f_\nu(60\ \mu\text{m})>50$ mJy. The area covered triples, in 20 different fields spread over the sky, the area of the HH survey, and the number of sources detected is about seven times that extracted by HH.

The differential number counts derived from the 20 FL fields at 60 μm, the most sensitive *IRAS* band for finding faint galaxies, are shown in Fig. 1. Only sources with SNR >5 and $f_\nu(60\ \mu\text{m})<400$ mJy are included; details are given in Table 2. The number counts were derived from all 20 fields, although, as indicated in Table 2, not all the fields had sufficient coverage to contribute to the counts with low flux densities. The uncertainties correspond to the estimated Poisson noise in the total counts in a particular bin of flux density. The last column in Table 2 is the reduced chi square derived from a comparison of the counts in the 20 separate fields. Variations exist in the different flux density bins which would be expected less than 5% of the time if the galaxies were uniformly distributed, but the chi squares are not so consistently in excess of unity to prove that there is large-scale structure in the distribution of the infrared selected galaxies.

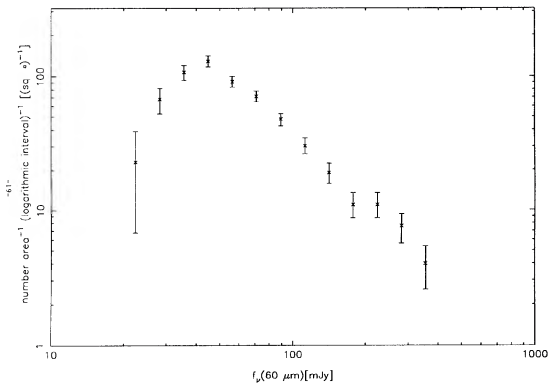

FIG. 1. The differential number counts $(\text{sq}^\circ)^{-1}$ (unit interval in $\log[f_\nu(60\ \mu\text{m})]$)$^{-1}$ are shown for the 20 FL samples with $|b|>25°$ and more than eight coverages for extractions with signal to noise ratios at 60 μm SNR >5. The uncertainties are based on the total number of objects in the bin.

At its lowest flux densities, the FL survey was clearly limited by confusion noise which is significantly larger than the instrumental noise as listed in Table 1. The confusion noise limit has been evaluated using the formalism described in HH resulting in a one σ confusion noise of 21 mJy. Because the analysis depends critically on arbitrary assumptions we have chosen to accept the completeness limit at 60 μm as ~50 mJy, the turnover from a power law in the log(number counts) versus log(flux density) relation of Fig. 1. It should be noted that with the effective beam size of ~5 sq′ there are ~25 beams source^{-1} for flux densities at 50 mJy, close to the commonly accepted criterion for the confusion limit.

5. DISCUSSION

One of the FL fields with high coverage, FL29, was studied in detail to verify that the faintest sources detected by *IRAS* are galaxies, and not, for instance, contamination by infrared cirrus, and to see if their properties are similar to those of the brighter galaxies observed by *IRAS*. The field FL29 was chosen as the field in the Northern hemisphere with the highest Galactic latitude as well as having high coverage (≥50 scans). In addition to the *IRAS* observations, visible wavelength images, and spectra and near-infrared and radio observations of this field were obtained. The observations, results, and analysis of FL29 are given in the Appendix.

In summary, the sources detected in FL29 with $f_\nu(60\ \mu\text{m})>50$ mJy, i.e., essentially the sources brighter than the confusion limit, are dusty galaxies with properties similar to those of other galaxies observed by *IRAS*. Perhaps the most distinguishing feature of these sources is their extreme redness in the near-infrared. Red-shifts measured of several of the sources are around $z\sim0.05$ with a small dispersion.

TABLE 2. *IRAS* FL mode statistics by flux density interval.

log(f_ν(60 μm)) mJy	Area sq °	No. Sources	No. Fields	Density [sq °]$^{-1}$[log(f_ν(60 μm))]$^{-1}$	reduced χ^2
1.35	0.88	2	11	22±16	0.09
1.45	3.13	21	14	66 14	0.77
1.55	6.32	67	19	106 12	1.04
1.65	10.07	130	20	129 11	0.61
1.75	14.20	130	20	91 8	1.54
1.85	17.39	124	20	71 6	0.86
1.95	19.06	91	20	47 5	1.48
2.05	19.71	60	20	30 3	1.55
2.15	19.90	38	20	19 3	1.47
2.25	19.96	22	20	11 2	1.07
2.35	19.98	22	20	11 2	1.55
2.45	19.99	15	20	7 1	1.07
2.55	20.00	8	20	4 1	1.63

One of the most interesting applications of the faint *IRAS* data is in understanding possible evolution of infrared emitting galaxies. In order to facilitate comparison with previous published work, the data of Fig. 1 were multiplied by a factor $[f_\nu(60\ \mu\text{m})]^{1.5}$. In an expanding universe with no evolution, this normalized differential number count should remain nearly level. Figure 2 shows the present data along with the similarly normalized data of HCH.

Figure 2 shows that the FL data lie systematically about a factor of 2 above the HCH data. Two evolutionary models, taken from HCH and fully described therein, are also included in Fig. 2. The lower (dashed) curve represents the number counts for a nonevolving model. The FL data deviate significantly from this model, and thus confirm the conclusion that the faint *IRAS* data do not support the predictions of a nonevolutionary model. The upper (solid) curve represents the model of Condon (1984) which fits the source counts due to spiral galaxies with flux densities at 1.4 GHz <5 mJy. The model represents almost pure luminosity evolution for redshifts less than $z\sim1.0$; Condon gives a full discussion. It is seen that the FL data are consistent with this model at flux densities below ~400 mJy, although deviations exist between the predictions and the infrared data above that flux density. This conclusion still is valid, although with less significance, if the cutoff chosen for the confusion noise is raised to, e.g., 70 mJy.

Based on the observed number counts at 60 μm it is possible to estimate the contribution of galaxies to the extragalactic background. Hacking & Soifer (1991) estimate this background to be ~0.1 MJy sr^{-1} at 60 μm, based on the 60 μm number counts of HCH. The present results, about a factor of 2 higher in number counts in a given flux density interval, would suggest a total extragalactic background at 60 μm of about 0.2 MJy sr^{-1}. This is substantially less than the darkest section of sky observed by COBE at 60 μm, 6 MJy sr^{-1}, reported by COBE (Hauser 1993). The limits on any potential extragalactic background are, however, roughly an order of magnitude lower than this measured background since foreground emission, e.g., zodiacal emission, is included (Hauser 1994) and the limits are only about twice the contribution from galaxies.

6. CONCLUSIONS

Source counts have been derived to 50 mJy using 746 sources derived from 20 FL pointed observations of *IRAS*. Observations of one selected field indicate that these sources, the faintest extracted from the *IRAS* data, are galaxies much like the bulk of infrared galaxies observed by *IRAS*. The differential source counts do not establish variations from field to field which are larger than the uncertainties derived from each field. The source counts are consistent with an evolutionary model that fits the observed radio source counts; they are inconsistent with a nonevolutionary model.

We thank the staff at IPAC for its support in the processing of these data and the *IRAS* Operations team for incorporating a new mode of observing well into the *IRAS* mission. We also thank the staff at Palomar for helping to obtain the

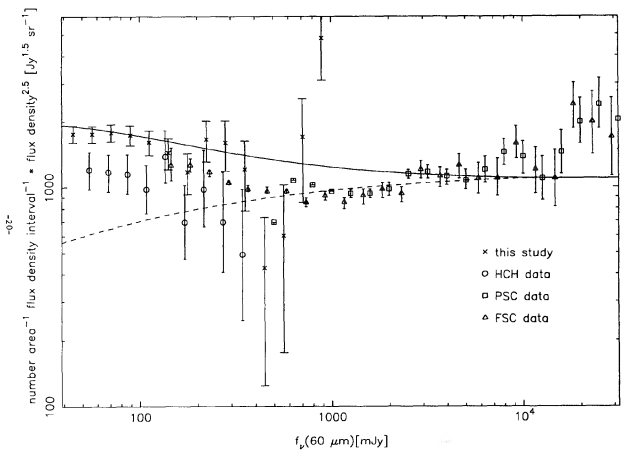

FIG. 2. The normalized differential number counts sr^{-1} [unit interval in $f_\nu(60\ \mu\text{m})^{-1}$ multiplied by $f_\nu(60\ \mu\text{m})^{2.5}$ is compared to the number counts derived by other surveys as noted. The dashed curve represents the predictions of a nonevolving universe, while the solid curve represents the best-fit curve to the radio observations (Condon 1984). Source counts from the *IRAS* Point Source Catalog (1985; hereafter referred to as PSC) for sources with $f_\nu(60\ \mu\text{m})>450$ mJy and for the FSS with $f_\nu(60\ \mu\text{m})>100$ mJy (Moshir *et al.* 1992; Saunders 1990) are also included.

visual and near-infrared observations. We especially thank Keith Matthews for his help with the observations and Perry Hacking for his help in sorting out the processing. We thank Dave Helfand for communicating his results to us prior to their publication, Mike Hauser for helpful discussion and Lee Armus for reading the manuscript. This work has been supported by grants from the NASA ADP program and from the National Science Foundation. We also thank Ms. Lydia H. Suarez for her help in preparing the manuscript.

APPENDIX: THE FL FIELD FL29

1. Observations

FL29 was centered at $17^h07^m47.0^s$, $+71°10'30''$ (1950), an area flagged as a "moderate cirrus" field, and consists of data from 53 pointed observations obtained throughout the latter half of the *IRAS* mission. A total of 240 detector tracks gave nearly uniform coverage over an area of 30 by 30′ in the center of the field as shown in Fig. 3. Sources were extracted from the 12, 25, 60 and 100 μm data. Calibration of the source intensities was checked against the PSC, the FSS, and the *IRAS* Serendipitous Survey Catalog (1986).

The central area of FL29 was imaged in the visible (Gunn *r*) with the "4-shooter" CCD camera mounted on the 200 in. Hale Telescope at Palomar Observatory. The exposures were limited to 5 min for each image; the limiting magnitude was $r\sim24$ mag. A mosaic of 18 images each $\sim9'$ by 9′ covered the area indicated in Fig. 3. Visual spectra of several of the sources identified in the CCD images were obtained with the Double Spectrograph of the 200 in. Telescope at a spectral resolution of 250.

A circular area with radius 15′ and its center chosen to coincide with the center of FL29 was observed in the 20 cm radio continuum with the C array of the VLA on 24 August 1985. After determining that there were no strong sources (>10 mJy) in the side lobes of the primary beam, the area was mapped with a bandwidth of 25 MHz over 15 h. The region surveyed is outlined in Fig. 3.

Several of the visual counterparts of the brightest 60 μm *IRAS* sources were also observed in the near-infrared at 1.25 μm (J), 1.65 μm (H), and 2.2 μm (K) using either a solid nitrogen cooled single element InSb detector mounted on the 200 in. Hale telescope with beam diameters between 5″ and 10″ or an InSb array camera also located at the Cassegrain focus of the 200 in. Telescope.

Independently, Hamilton & Helfand (1993) studied the EINSTEIN Observatory Draco Deep X-ray Survey (Giacconi *et al.* 1979) which covered an area about 0.5 sq° centered at 17^h10^m, $+71°10'$. Hamilton and Helfand surveyed essentially the same area with the VLA looking for the positions

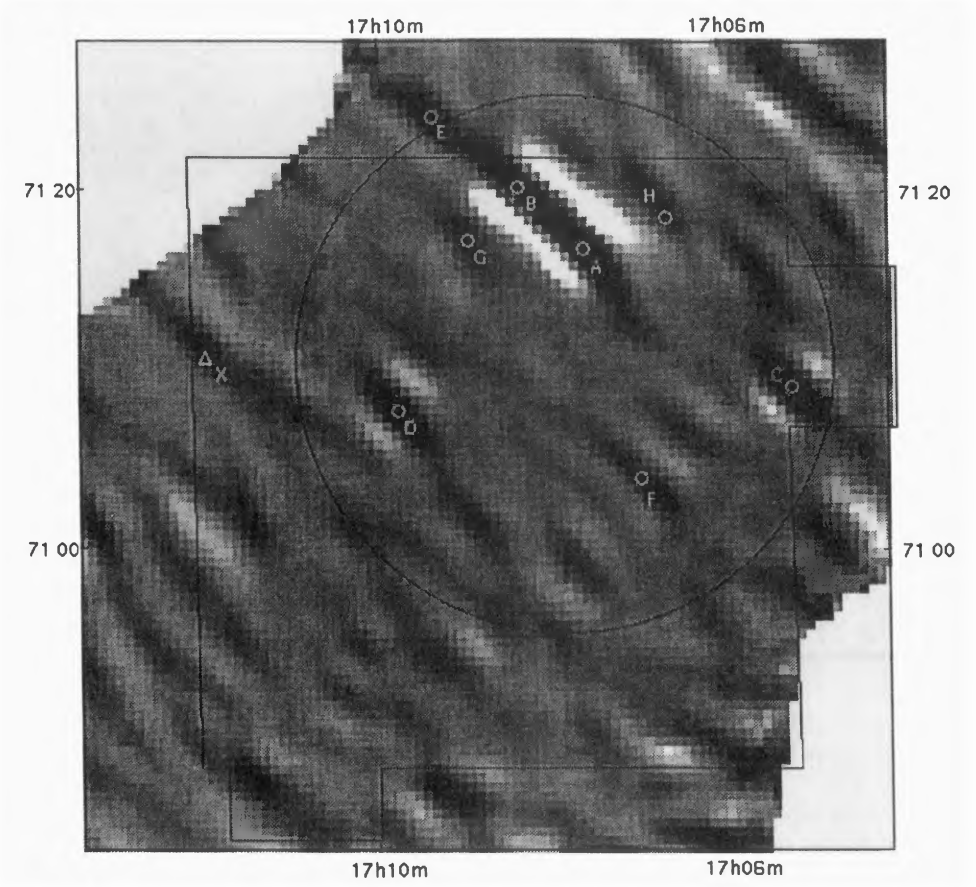

FIG. 3. (a) A greyscale image of the coadded filtered data in the central area of FL29 is shown with black positive and white negative. North is up and East is to the left; the pixels are 0.5′×0.5′. The full FL29 area is about 2.5 times that shown by the gray scale and extends to the Northwest and Southeast. The inside solid lines represent the boundaries of the mosaic of CCD images while the large black circle represents the boundary of the radio survey. The locations of the 60 μm extractions with $f_\nu(60\ \mu m)>50$ mJy are designated with small white circles and the appropriate letters; the 25 μm position is shown for FL29-H. The 100 μm position for FL29-X is shown with a small white triangle.

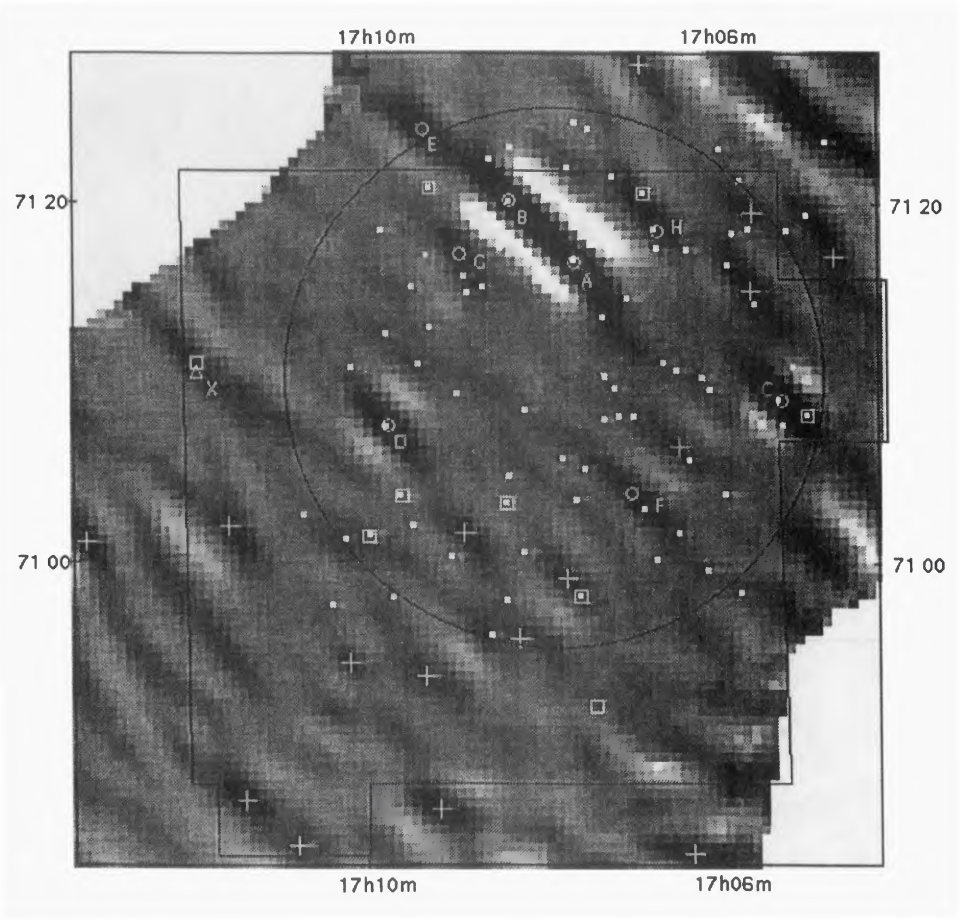

FIG. 3. (b) The same greyscale image of the coadded filtered data in the central area of FL29 is shown. The locations of the 60 μm extractions with f_ν(60 μm)>50 mJy are again shown by small white circles; the locations of the 60 μm extractions with f_ν(60 μm)<50 mJy are indicated by white "plus" signs. Small white solid squares show the positions of the radio sources, and the slightly larger white open squares show the positions of the X-ray fluctuations (Hamilton & Helfand 1993). Note that FL29-X, the white triangle, is not accompanied by a radio source since it was detected in the VLA survey of Hamilton and Helfand rather than the survey described here. See Tables 3 and 4 and the text.

of radio sources which could be correlated with spatial fluctuations in the X-ray background. Whenever there is an overlap between Hamilton and Helfand's radio survey and that indicated by the circle in Fig. 3, the agreement is excellent.

2. Results

There are 32 sources in FL29 with f_ν(60 μm)>50 mJy. The central section of FL29 contains eight detections with f_ν(60 μm)>50 mJy and 18 detections with f_ν(60 μm)>30 mJy or five times the 1σ instrumental noise of 6.0 mJy. The *IRAS* observations of the brightest eight sources are given in Table 3. Figure 3 shows the 60 μm extractions with a signal to noise ratio (SNR) >5; the eight sources with f_ν(60 μm)>50 mJy are labeled in Fig. 3(a).

The 1σ levels for the instrumental noise at 12, 25, and 100 μm are 3.6, 3.9, and 20.1 mJy. The confusion limit at 60 μm, as determined using the formalism of HH, is around 50–60 mJy and the corresponding limits at 12, 25, and 100 μm are approximately 25, 25, and 100 mJy. The 12 μm data have five detections with signal to instrumental noise ratio (SNR) >5, two of which can clearly be identified with stars. The 25 and 100 μm maps have, respectively, four and eight detections with SNR >5. The typical beam profile resulting from the filtering, an ellipse ~2.3′ by 4.7′, is evident for the brightest sources shown in Fig. 3; the uncertainties in the final *IRAS* positions are estimated as between 10″ and 20″.

Several galaxies were generally present on the visual CCD images within the *IRAS* position uncertainty ellipse, too many for a confident association with the infrared source. Radio emission was thus relied upon for more positive identifications. The area surveyed by the VLA has a RMS noise of 25 μJy at 20 cm and contains 77 radio sources with SNR >5; the positions of these sources are shown in Fig. 3(b). The positions of sources extracted from the FL29 field at 60 μm, were compared first to the radio maps from the VLA and then to the visual images in order to identify individual counterparts. If the mean relationship between the radio and far-infrared emission found by Helou *et al.* (1985) obtains, sources with f_ν(60 μm)>5 mJy, well below the confusion noise limit, should have been detected with ~1σ in the radio survey. In fact, only six of the eight 60 μm extractions with f_ν(60 μm)>50 mJy could sensibly be identified with radio counterparts. FL29-E lies outside the radio survey. The position of FL29-G was obscured by the bright sources FL29-A and FL29-B; there are too many radio sources in the vicinity of FL29-G to make a confident association. Although the displacement of the radio position from the infrared extraction of FL29-F is relatively large, ~1.1′, we feel its identification is secure because of its relative isolation. We have

TABLE 3. *IRAS* observations.

Object	ra 1950	dec 1950	f_ν(12 μm) mJy	f_ν(25 μm) mJy	f_ν(60 μm) mJy	f_ν(100 μm) mJy
A	17 07 37.0	71 16 59	14	<12	226	537
B	17 08 20.6	71 20 24	19	21	209	574
C	17 05 13.5	71 09 11	<11	20	162	230
D	17 09 45.6	71 07 50	12	16	96	204
E	17 09 21.6	71 24 19	<11	<12	84	275
F	17 06 58.7	71 04 07	<11	<12	58	173
G^b	17 08 56.3	71 17 24	14	<12	56	-
$H^{b,c}$	17 06 38.6	71 18 38	<11	15	51	-

Comments

a) The uncertainties in the IRAS positions and flux densities depend on many factors including mainly the coverage, the source strength and proximity to nearby strong sources. For FL29, the position uncertainties are estimated to be between 10" and 20". The 1 σ uncertainties in the IRAS flux densities are typically 4, 4, 6 and 20 mJy at 12, 25, 60 and 100 μm. The extractions at 12, 25 and 100 μm were determined for the existing 60 μm sources and are not restricted to a SNR > 5; the detection limits at these wavelengths are quoted as 3 σ.

b) Sources FL29-G and FL-29-H are in the side lobes of sources A and B and thus their positions are unreliable and no 100 μm flux densities could be extracted.

c) The position of source FL29-H at 25 μm, where the beam size is cut by two, is given. It differs from the position of the 60 μm extraction by 1.6'.

generally not attempted to identify the sources with f_ν(60 μm)<50 mJy since the positional uncertainties in the *IRAS* data become rapidly worse below the confusion limit.

A galaxy was identified on either the visual or near-infrared image near the radio positions associated with each of the *IRAS* source identifications discussed above. For FL29-A to FL29-D, the visual CCD imaging clearly showed a galaxy close to the radio positions. Near-infrared imaging confirmed that counterparts close to the radio positions identified with sources FL29-E, FL29-F, and FL29-H are, in fact, galaxies.

The red-shifts from the visual spectra are included in Table 4; the mean red-shift of those measured is $z=0.053$. In addition, the spectrum of a galaxy lying between FL29-A

TABLE 4. Ground-based observations.

Object	VLA[a] Δ(ra) "	VLA [a] Δ(dec) "	VLA [b] f_ν(20 cm) mJy	z	K [c] mag	H-K mag	J-H mag
A	-2	1	1.63	0.056	13.70	0.62	0.86
B	2	-9	1.83	0.042	13.18	0.21	0.76
C^d	12	0	1.91	0.061	13.75	0.45	0.68
D	6	4	0.56	0.054	13.61	0.41	0.66
E	3	-5	-	-	16.24	0.71	0.66
F	-45	-53	0.45	-	15.21	0.86	0.86
H	10	8	0.16	-	14.11	0.41	0.66

Comments

a) The coordinate differences (Δ) are given as the VLA 20 cm position minus the IRAS 60 μm position with the exception of FL29-E, which lies outside the radio survey. For this source, the diifference between the near-infrared and IRAS positions is given.

b) The 1 σ uncertainties in the VLA 20 cm flux densities are typically 25 μJy.

c) The uncertainties in the near infrared flux densities are typically less than 0.05 mag.

d) There are three galaxies evident on the visual CCD images within about 5' of each other and well within the uncertainty ellipse of IRAS source C. The identification of the galaxy measured is primarily on the basis of the VLA 20 cm position.

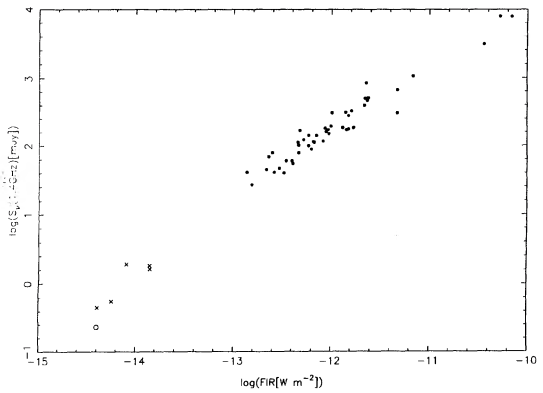

FIG. 4. The flux density at 1.4 GHz for a sample of galaxies is plotted against the far-infrared flux derived as explained in the text. The crosses represent the galaxies in FL29 with $f_\nu(60\ \mu m)>50$ mJy while the dots represent the data for a sample of bright galaxies, largely spirals, from Helou *et al.* (1985). The open circle represents FL29-X. It is seen that the FL29 galaxies continue the relationship formed by the spiral galaxies although to lower flux values.

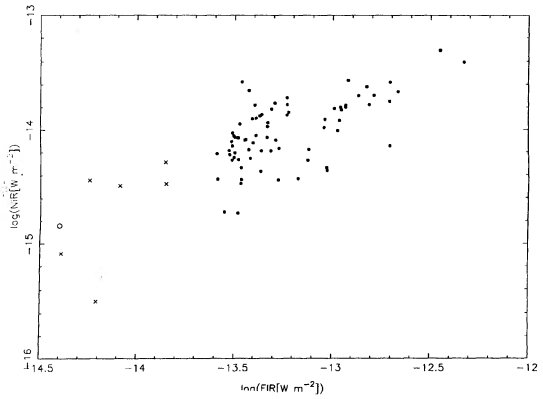

FIG. 5. The near-infrared flux, defined as the flux at 5 $f_\nu(2.2\ \mu m)$ is plotted against the far-infrared flux, as defined in the text, for the FL29 galaxies with $f_\nu(60\ \mu m)>50$ mJy (crosses) and the *IRAS* mini-survey galaxies (Soifer *et al.* 1984; Carico *et al.* 1986; dots). The open circle represents FL29-X. The FL29 galaxies form an extension of the mini-survey galaxies to lower fluxes and thus confirm the association between the optical/near-infrared images and the *IRAS* extractions.

and FL29-B showed its red-shift to be 0.041. The near-infrared magnitudes and colors of the sources identified with the brightest infrared sources are also listed in Table 4.

3. Discussion

Helou *et al.* (1985) and DeJong *et al.* (1985) have found that a tight linear correlation exists between the far-infrared flux measured by *IRAS* and the nonthermal radio flux density at 1.4 GHz from disks of spiral galaxies. Following Helou *et al.*, measurements from the 60 and 100 μm bands were combined to estimate the far-infrared flux (FIR) between 42 and 122 μm where

$$\mathrm{FIR}=1.26\times10^{-17}[2.58f_\nu(60\ \mu m)+f_\nu(100\ \mu m)];$$

FIR is in W m^{-2} if $f_\nu(60\ \mu m)$ and $f_\nu(100\ \mu m)$ are the flux densities at 60 and 100 μm in mJy. The fluxes of the FL29 galaxies are shown in Fig. 4 as a function of radio flux density along with the sample of galaxies described by Helou *et al.* It is seen that the FL29 galaxies obey the same law as do the brighter galaxies, but extend the relationship to fainter fluxes. Thus, Fig. 4 strongly establishes the association between the radio sources and the infrared sources of FL29.

In Fig. 5 the flux at 2.2 μm is compared to FIR for the FL29 galaxies as well as for the *IRAS* mini-survey galaxies (Rowan-Robinson *et al.* 1984; Soifer *et al.* 1984) as measured by Carico *et al.* (1986). The K magnitudes obtained from Table 4 have been corrected for Galactic reddening and the red-shift of the galaxy (the K correction) following the precepts outlined by Carico *et al.* These corrections are typically <0.1 mag.

The near-infrared colors of the counterparts to the brightest sources in FL29 are included in Fig. 6, as well as the colors for the *IRAS* mini-survey galaxies (Carico *et al.* 1986; Soifer *et al.* 1984). Again, the colors obtained have been corrected for Galactic reddening and the galactic red-shift. The line on the bottom right of the figure indicates the locus of the normal extinction law for $A_v=1$ mag (Rieke & Lebofsky 1985). The FL29 sources are all consistent with their being galaxies, but lie at the reddest extremes of galaxies seen in the *IRAS* mini-survey. Three are redder than can be explained by extinction alone; their colors probably represent the onset of thermal emission near 2 μm.

Figure 7 shows the distribution of the total luminosities of the six brightest (at 60 μm) FL29 galaxies and of the *IRAS* mini-survey galaxies. The far-infrared flux FIR defined above was increased by a factor of 1.5 in order to approximate the total infrared flux of the galaxies following the ideas expressed in Helou *et al.* (1988). The red-shifts of the FL29-E and FL29-F were assumed to be 0.053. The galaxies observed in FL29 populate the lower luminosities of the

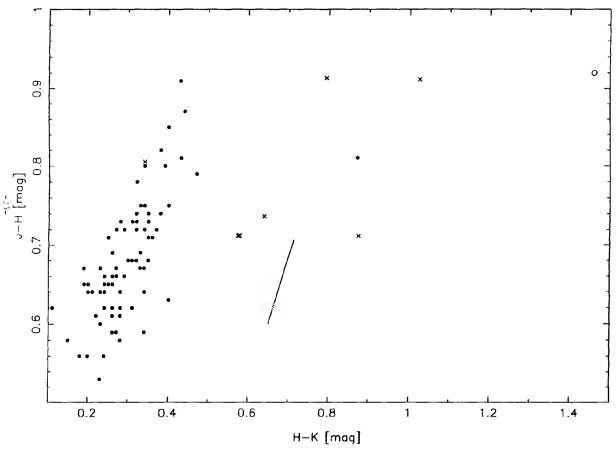

FIG. 6. A color–color diagram is shown for the near-infrared colors of the FL29 galaxies with $f_\nu(60\ \mu m)>50$ mJy (crosses) and the *IRAS* mini-survey galaxies (Soifer *et al.* 1965; Carico *et al.* 1986; dots). The open circle represents FL29-X. The near-infrared magnitudes have been corrected for Galactic absorption and the galaxy red-shift (the K correction) following Carico *et al.* The solid line corresponds to one visual magnitude of extinction. The location of the FL29 galaxies on this plot most likely indicates the presence of thermal emission from dust in the galaxies and marks the feature that probably most distinguishes the FL29 galaxies.

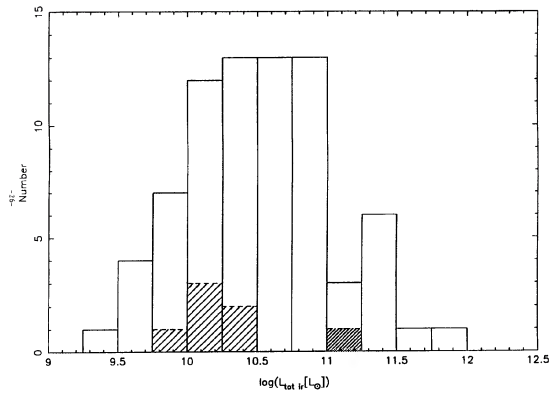

FIG. 7. The histogram gives the distribution of the total far-infrared luminosity as defined in the text for the FL29 galaxies with $f_\nu(60\ \mu m)>50$ mJy (wider hatching) and the *IRAS* mini-survey galaxies (Soifer *et al.* 1984; Carico *et al.* 1986; open). The fine hatching represents FL29-X. The luminosities of the FL galaxies are not atypical of those of the *IRAS* galaxies as a whole, but are among the less luminous infrared galaxies.

spread observed in the mini-survey sample. A further comparison between the distribution of far-infrared luminosities of the galaxies found in the mini-survey and those included in the Bright Galaxy Sample (BGS) of Soifer *et al.* (1987) indicates that these two distributions are essentially the same.

4. A Possible X-Ray/Radio/Far-Infrared Galaxy

A comparison of the radio and X-ray data analyzed by Hamilton & Helfand (1993) yielded nine statistically significant positive X-ray fluctuations which could be associated with radio sources; these are shown in Fig. 3(b). None of the nine radio positions are associated with a far-infrared (FL) source having $f_\nu(60\ \mu m)>50$ mJy.

The brightest X-ray fluctuation in the area surveyed that can be associated with a radio source is at $17^h11^m\ 59.3^s$, $+71°11'17''$ (1950) and is within 1.6′ of a 60 μm extraction from FL29 with $f_\nu(60\ \mu m)=44.7$ mJy and within 0.5′ of a 100 μm extraction with $f_\nu(100\ \mu m)=200$ mJy. Although the infrared source is clearly below the *IRAS* confusion limit, it is relatively isolated. The source is at the edge of the field in a region where the coverage fraction has a very strong gradient. Although the flux extractor was insensitive to such gradients, the position extractor was extremely sensitive to this gradient. The derived 60 μm position was more strongly affected than the 100 μm location because of the detailed arrangement of the detectors. When the number of scans was adjusted to give a more uniform, although sparser, coverage, the 60 μm position which resulted agreed with the 100 μm position and the radio position within 0.5′.

It is tempting to associate the 60 and 100 μm extractions with the same infrared source, although the identification is by no means certain, and we henceforth identify this source as FL29-X. The visual CCD image shows a galaxy image within a few arcsec of the radio position for which subsequent spectroscopy showed a red-shift of 0.278 and a spectrum which is typical of an AGN. The relevant quantities for this object are included in the figures. It is seen that all the diagnostic parameters are consistent with the association of the far-infrared, the optical, and the radio sources.

FL29-X is by far the reddest of the FL29 sources in the near-infrared; $K=15.05\pm0.08$ mag, $H-K=0.85\pm0.12$ mag, and $J-H=0.81\pm0.12$ mag. It lies in the area of the color–color diagram populated by some Seyfert 2 galaxies and AGNs (see e.g., Mazzarella *et al.* 1991). Hamilton & Helfand (1993) discuss the possibility that fluctuations in the X-ray background stronger than 10^{-11} W m^{-2} are associated with AGNs; these observations give support to this premise.

REFERENCES

Beichman, C. A., Neugebauer, G., Habing, H. J., Clegg, P. E., & Chester, T. J. 1985, Infrared Astronomical Satellite (IRAS) Catalog and Atlases, Explanatory Supplement (GPO, Washington, DC)

Carico, D. P., Soifer, B. T., Beichman, C., Elias, J. H., Matthews, K., & Neugebauer, G. 1986, AJ, 92, 1254

Condon, J. J. 1984, ApJ, 287, 461

de Jong, T., Klein, U., Wielebinski, R., & Wunderlich, E. 1985, A&A, 147, L6

Elias, J. H., Barrientos, L. F., Hacking, P., Neugebauer, G., & Soifer, B. T. 1993, in Sky Surveys: Protostars to Protogalaxies, edited by B. T. Soifer (ASP, San Francisco), Vol. 43, p. 111

Giacconi, R., *et al.* 1979, ApJ, 234, L1

Hacking, P., Condon, J. J., & Houck, J. R. 1987, ApJ, 316, L15

Hacking, P., & Houck, J. R. 1987, ApJ, 63, 311

Hacking, P. B., & Soifer, B. T. 1991, ApJ, 367, L49

Hamilton, T. T., & Helfand, D. J. 1993, ApJ, 418, 55

Hauser, M. G. 1993, in Extragalactic Background Radiation, Space Telescope Science Institute Symposium Series, edited by D. Calzetti, M. Livio, and P. Madau (Cambridge University Press, Baltimore), Vol. 7, p. 135

Hauser, M. G. 1994, in Examining the Big Bang and Diffuse Background Radiation IAU Symposium No. 168 (in press)

Helou, G., Khan, I., Malek, L., & Boemer, L. 1988, ApJ, 68, 151

Helou, G. H., Soifer, B. T., & Rowan-Robinson, M. 1985, ApJ, 298, L7

Joint IRAS Science Team. 1985, IRAS Point Source Catalog, Version 2 (U.S. GPO, Washington, DC)

Kleinmann, S. G., Cutrie, R. M., Young, E. T., Low, F. J., & Gillett, F. C. 1986, Explanatory Supplement to the IRAS Serendipitous Survey Catalog (JPL, Pasadena, CA)

Lonsdale, C. J., & Hacking, P. B. 1989, ApJ, 339, 712

Lonsdale, C. J., Hacking, P. B., Conrow, T. P., Rowan-Robinson, M. 1990, ApJ, 358, 60

Low, F. J., *et al.* 1984, ApJ, 278, L19

Mazzarella, J. M., Gaume, R. A., Soifer, B. T., Graham, J. R., Neugebauer, G., & Matthews, K. 1991, AJ, 102, 1241

Moshir, M., *et al.* 1992, Explanatory Supplement to the IRAS Faint Source Survey, Version 2 (JPL, Pasadena, CA), D-10015 8/92

Rieke, G. H., & Lebofsky, M. J. 1985, ApJ, 288, 618

Rowan-Robinson, M., *et al.* 1984, ApJ, 278, L7

Saunders, W. 1990, Ph.D. thesis, Statistical Cosmology with IRAS Galaxies: The Large Scale Structure and Evolution of the Universe (Queen Mary College, University of London)

Soifer, B. T., *et al.* 1984, ApJ, 278, L71

Soifer, B. T., Sanders, D. B., Madore, B. F., Neugebauer, G., Danielson, G. E., Elias, J. H., Lonsdale, C. J., & Rice, W. L. 1987, ApJ, 320, 238

Young, E. T., Neugebauer, G., Kopan, E. G., Benson, R. D., Conrow, T. P., Rice, W. L., & Gregorich, D. T. 1985, User's Guide to IRAS Pointed Observations (JPL, Pasadena)